

Sonochemical Synthesis, Characterization and Gas Sensing Properties of NiO Nanoparticles

Mahdieh Ghobadifard¹, Maryam Mahmoudi¹, Mostafa Khelghati¹, Ghasem Maleki¹, Saeid Farhadi¹ and Alireza Aslani^{1,2,*}.

¹Department of Chemistry, University of Lorestan, Lorestan-Khoramabad 68135-465, Iran.

²Nanobiotechnology Research Center, Baqiyatallah University Medical of Science, Tehran, Iran.

Received: 21 Feb. 2015, Revised: 22 Mar. 2015, Accepted: 24 Mar. 2015.

Published online: 1 Sep. 2015.

Abstract: Nanoparticles of NiO (NP-NiO) were prepared by a novel sonochemical route from Ni acetate and sodium hydroxide without any requirement of calcinations steps at high temperature and without surfactants. Drop casting of the Nano crystals onto alumina substrates allowed the fabrication of gas sensing devices, which were tested towards NO₂ and CO and showed promising results. At low working temperature, the NiO nanoparticles based sensors are selective to nitrogen oxide; in fact a good sensitivity is shown at 200 °C at low concentration (2 ppm), while at temperature above 350 °C, high responses are obtained for carbon monoxide. The results obtained are stimulating for further developing of nano-NiO based sensor devices.

Keywords: NiO nanoparticles, NO₂, CO, gas sensor.

1 Introduction

Nano-materials are at the leading edge of rapidly developing field of nanotechnology [1-4]. A reduction in particle size to nanometer scale results in various special and interesting properties compared to their bulk properties. Metal oxide materials, specifically materials with Nano-scale features, have been the subject of numerous research efforts in fields such as gas sensors [5, 6], fuel cells [7], solar cells [8, 9] and electrodes for lithium ion batteries [10] to name a few. Ultra-fine NiO Nano-ceramic particles with a uniform size and well dispersion characteristics are strongly desirable for many applications, e.g. Synthesis of composite materials, magnetic, electro chromic, heterogeneous catalytic materials, sensors etc. In addition, important applications of NiO include preparation of cathode materials of alkaline batteries, anti-ferromagnetic layers, and p-type transparent conducting films [11]. Nano-structured nickel (II) oxide is a p-type semiconductor metal oxide having a stable wide band gap. Also it can be used as a transparent p-type semiconductor layer [12]. Furthermore, it exhibits anodic electrochromism and is utilized for applications in smart windows, electrochemical super-capacitors [9, 10], and dye-sensitized photo cathodes [13]. However, the functional properties of NiO vis-a-vis its applicability significantly depend on pore morphology, pore matrix-interface, and also porosity. For example, in catalytic applications the available specific surface area should be as high as possible while for the application as a cathode material, a dense material is desirable. Initial virgin powder possesses large surface area relative to its volume. This surface area/surface energy provides the driving force for sintering, i.e., reduction of free surface energy resulting from the high surface area of particles [14].

Recently, the sonochemical methods have been shown to be very promising in the preparation of a variety of materials with nanometer dimensions, including nano-chalcogenides [15, 16], metallic nanoparticles [17, 18] and Nano-sized metal oxides [19, 20]. These materials possess improved magnetic properties [21], energy storage capacities [22-24], photocatalytic [25] and catalytic properties [26].

On the other hand several semiconducting metal oxides such as NiO have attracted the attention of numerous researchers interested in gas sensors, due to their typical surface properties suitable for gas detection. The gas sensing mechanism is based on several gas/semiconductor surface interactions including reduction/oxidation processes of the semiconductor,

*Corresponding author e-mail: a.aslani110@yahoo.com

adsorption of the chemical species directly on the semiconductor and complex surface chemical reactions among the different adsorbed chemical species [27, 29].

The effect of these surface phenomena is a reversible and significant change in electrical resistance (i.e. a resistance increase or decrease under exposure to oxidizing respectively reducing gases referring as example to an n-type and p-type semiconductor oxide). This resistance variation can be easily observed and used to detect chemical species in the ambient. One of the most promising approaches for the realization of high performance gas sensors is the development of nanostructured sensing materials [30, 32]. Several articles have shown the advantage of reducing the metal oxide grain size down to nanometer scale in order to improve the sensing properties (mainly sensitivity and selectivity), as well as stability over time of the oxide layer [33, 34]. Indeed, such nanostructured semiconductor oxides offer some advantages: a large surface-to-volume ratio, the realization of single crystalline structures and a grain size which is comparable to the depth of the space-charge layer that surrounds the nanograin. The interaction of gaseous species with oxide nanoparticles may give rise to high and fast responses in term of changes in the electrical properties of the sensing materials [35]. NiO has been intensely studied for its versatile physical properties and characterized in literature as gas sensing material showing good stability and gas sensing properties to a wide range of chemical compounds. Recently, substantial efforts have been devoted to realize NiO-nanostructured materials in order to improve the performances of NiO based sensor devices [36, 37]. A large number of works has been so far directed to investigating the effect of Nano-sized on the sensing properties of the NiO small size particles. In the last years, substantial progress was made in the preparation of Nano-crystalline metal oxide particles with diameters smaller than 10 nm [38, 39] by using various techniques as CVD (chemical vapor deposition), MOCVD (metal oxide chemical vapor deposition), wet chemical synthesis, thermal evaporation and template-based growth.

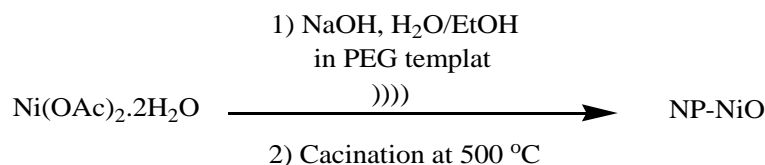
In this work, we synthesized NiO Nano-sized particles (NiO-NP) by using a simple sonochemical method for the preparation of NiO nanoparticles directly without any additive from nickel acetate solutions. NiO-NP based chemoresistive gas sensors were realized and gas sensing tests towards NO₂ and CO were performed, showing promising results compared with the NiO thin films gas sensors.

2 Experimental

Typical procedure for preparation of NiO nanoparticles: NaOH solution with a concentration of 0.1 M (100 ml) were added to the 0.1 and 0.2 M solutions of Ni(CH₃COO)₂·2H₂O in ethanol/water. To investigate the role of surfactants on the size and morphology of nanoparticles, we used 0.5 ml of polyethylene glycol (PEG) in the reaction with optimized conditions. The mixtures were sonicated for 0.5, 1 and 2 hr, with different ultrasound powers followed by centrifugation and separation of the solid and liquid phases. The solid phase was washed for three times ethanol and water. Finally, the washed solid phase was calcinated at 500 °C for 30 min. Table 1 shows the conditions of reactions in detail. A multiwave ultrasonic generator (Bandlin Sonopuls Gerate-Typ: UW 3200, Germany) equipped with a converter/transducer and titanium oscillator (horn), 12.5 mm in diameter, operating at 30 kHz with a maximum power output of 780 W, was used for the ultrasonic irradiation. The ultrasonic generator automatically adjusted the power level. The wave amplitude in each experiment was adjusted as needed. X-ray powder diffraction (XRD) measurements were performed using a Philips diffractometer of X'pert Company with mono chromatized CuK α radiation. The samples were characterized with a scanning electron microscope (SEM) (Philips XL 30) with gold coating. To investigate the size distribution of the nanoparticles, a particle size histogram was prepared for NiO nanoparticles. For further demonstration, the EDAX was performed for the NiO nanoparticles. For the preparation of the sensors, we used alumina substrate composed by a matrix of 225 single devices of (2 × 2) mm each and 350 μ m thick equipped with Pt heating elements on the back side and with Pt interdigitated contact on the front size realized by means of a standard photolithographic process. The micro-sensors were heated at different operating temperature by supplying a given voltage to the heating element. The sensor responses towards gases and vapors were carried out by applying a constant voltage of 4V, between the sensor electrodes, and monitoring the current by means of a picoamperometer. A pre-aging thermal treatment has been carried out at 400 °C for some hours in order to optimize the stability of the sensing element. They were exposed to different NO₂ and CO concentrations. The desired gases concentrations were obtained starting from certified cylinders by means of a mass flow controller (MKS mod. 647B) and of mass flow meters. A total flow of 100 sccm was fixed during the measurements. The sensors responses were calculated as (I_{air} - I_{gas})/I_{gas} where I_{air} and I_{gas} are the electrical current in dry-air and in the mixture of dry-air and gas, respectively, in the case of oxidizing gases and the reverse (I_{gas} - I_{air})/I_{gas} in the case of reducing gases.

3 Results

The reaction between Ni acetate and sodium hydroxide to form NiO nanoparticles has been shown in scheme 1.



Scheme 1. The reaction between Ni acetate and sodium hydroxide to form NiO nanoparticles.

Various conditions for preparation of NiO Nano-structures were summarized in Table 1.

Table 1: Experimental conditions for the preparation of NiO nanoparticles.

Sample	Ni(AC) ₂	NaOH (0.1 M)	Ageing time	Ultrasound power	Average size
1	25 ml (0.2 M)	100 ml	0.5 hr	6- 9 W	150 nm
2	25 ml (0.2 M)	100 ml	1 hr	9- 12 W	120 nm
3	25 ml (0.2 M)	100 ml	2 hr	12- 18 W	100 nm
4	50 ml (0.1 M)	100 ml	2 hr	12- 18 W	60 nm
5	50 ml (0.1 M)	100 ml	3 hr	12- 18 W	20 nm

The best morphology with smaller particles and good distribution was obtained for the samples summarized.

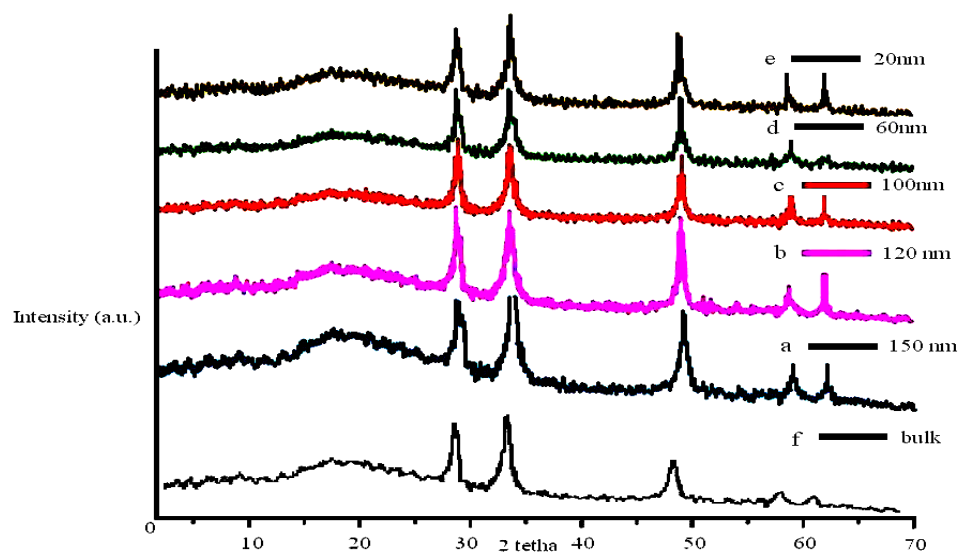


Figure. 1. The X- ray powder diffraction pattern of NiO nanoparticles (a) NiO at 150 nm, (b) NiO at 120 nm, (c) NiO at 100 nm, (d) NiO at 60 nm, (e) NiO at 20 nm and (f) NiO at bulk size.

Fig 1 (a, b, c, d, e and f) shows the XRD patterns of the direct sonochemically synthesized of the NiO nanoparticles respectively. Sharp diffraction peaks shown in Figure. 1 indicates good crystalline of NiO nanoparticles. No characteristic peak related to any impurity was observed. The broadening of the peaks indicated that the particles were of nanometer scale.

The morphology, structure and size of the samples are investigated by scanning electron microscopy (SEM). Fig 2 (a, b, c, d and e) indicates that the original morphology of the NiO nanoparticles are approximately spherical with the diameter varying between 10 to 200 nm.

To investigate the size distribution of the nanoparticles, a particle size histogram was prepared for NiO nanoparticles, Fig. 3 (a, b, c, d and e). For further demonstration the EDAX was performed for the NiO nanoparticles. The EDAX spectrum given in Fig. 4 (a, b, c, d and e) shows the presence of Ni as the only elementary component in the NiO nanoparticles respectively.

The solid state UV-vis spectra of nanoparticles as well as of NiO at bulk size were studied. The solid state UV-vis spectrum of nanoparticles and NiO at bulk size displays an absorption band with maximum intensity at 360 nm Fig. 5 (a, b, c, d, e and f) whereas NiO nanoparticles displays one absorption sharp bands with maximum intensity at 365 nm. But the bulks NiO powder have very limited UV absorbance, and absorbance in the UV region is enhanced with the NiO nanoparticles at different size due to its high energy gap.

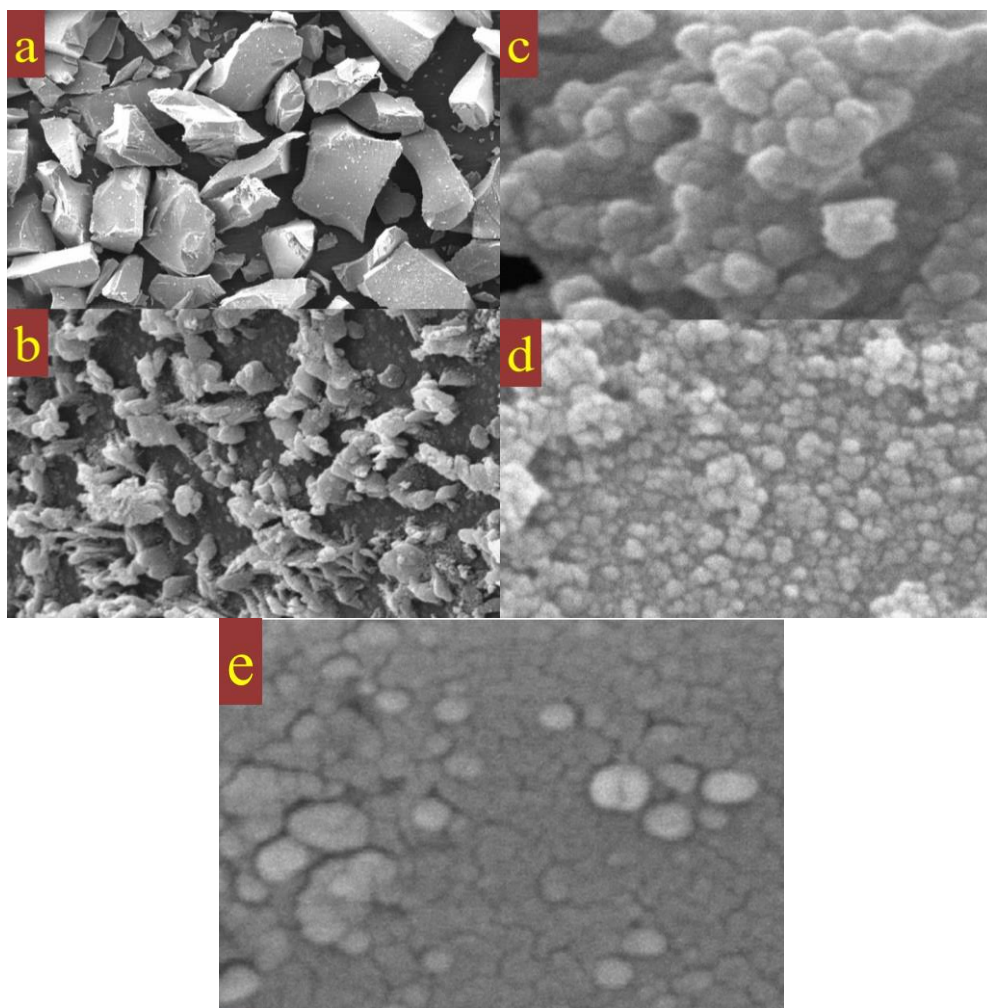


Figure 2. Typical SEM micrographs of NiO nanoparticles at (a) 150 nm, (b) 120 nm, (c) 100 nm, (d) 60 nm and (e) 20 nm after calcinations.

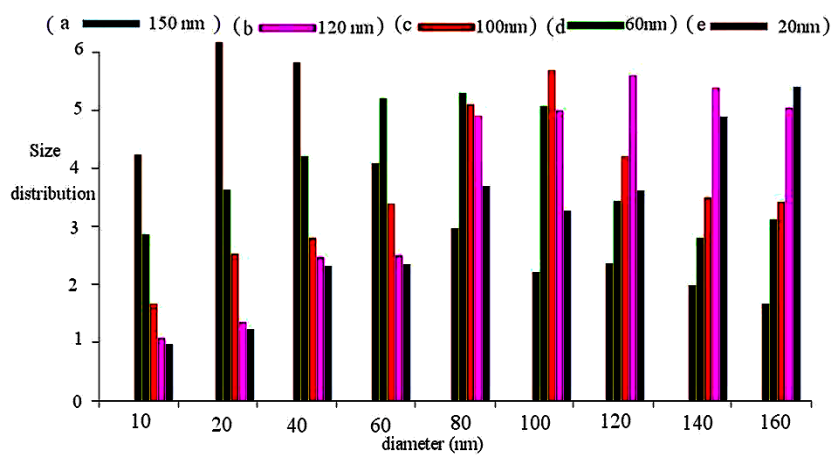


Figure 3. Particle size histogram of NiO with different size (a) 150 nm, (b) 120 nm, (c) 100 nm, (d) 60 nm and (e) 20 nm.

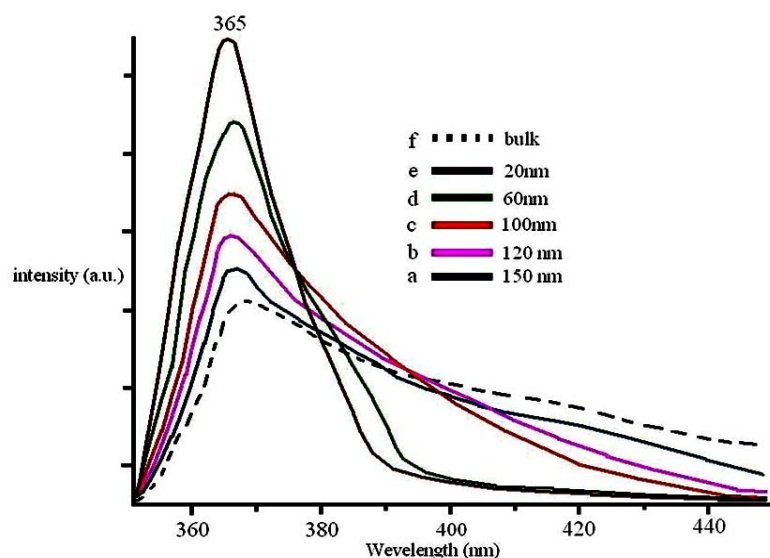


Figure 4. The EDAX analysis of NiO nanoparticles and bulk size (a) 150 nm, (b) 120 nm, (c) 100 nm, (d) 60 nm, (e) 20 nm and (f) bulk size.

Nanoparticles under 200 nm have better transmission of visible light compared to NiO at bulk size.

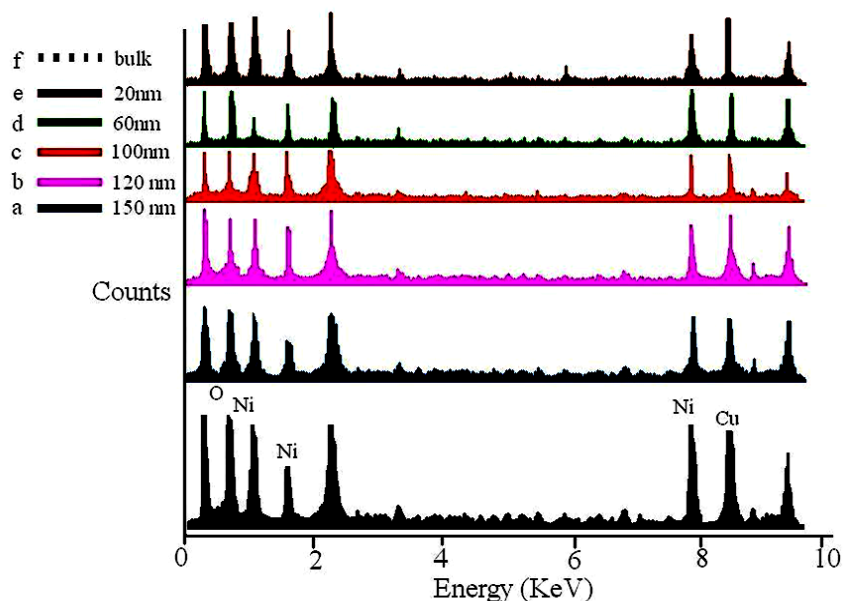


Figure 5. The solid state UV absorption of NiO nanoparticles at different size (a) 150 nm, (b) 120 nm, (c) 100 nm, (d) 60 nm, (e) 20 nm and (f) bulk size.

The sensing properties of NiO quantum Dots based sensors were evaluated by exposing them to three different gases: NO₂ (5-100 ppm) and CO (10-100 ppm). Tests were made at different temperatures in order to find the optimum operating temperature for each gas. In order to obtain a calibration curve tests were performed for different concentrations of each analytic gas. Fig. 6 reports the relations between working temperature and response toward different gases for a settled concentration of each target gas.

The sensors responses have been calculated as $(I_{\text{air}} - I_{\text{gas}}/I_{\text{gas}})$, where I_{air} and I_{gas} are the electrical current of the sensor in air and in the mixture of the gas and the air, respectively. As shown in Fig. 6, the response of the NiO-NP based sensor for NO₂ is greater than for the other gases and a good sensitivity is shown towards NO₂ at low concentration (5 ppm) and at low temperature. The best responses towards NO₂ were obtained at 200 °C. At higher temperatures a significant decrease of the sensor responses takes place. In this way, at working temperature below to 300 °C, the NiO-NP sensor is selective to nitrogen oxide, while at temperature above 350 °C carbon monoxide responses further increase.

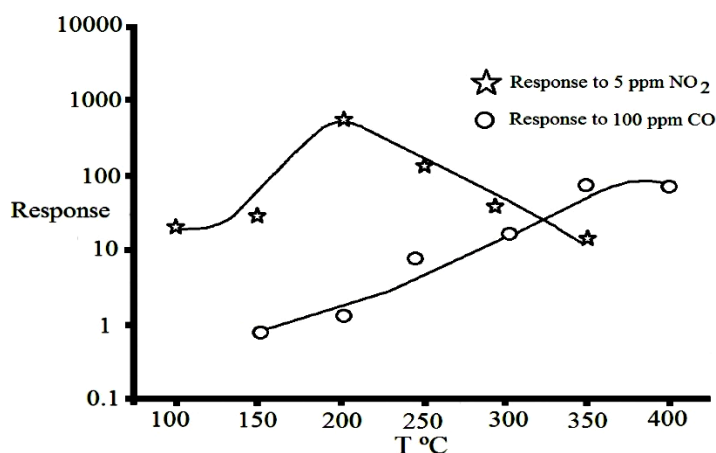


Figure 6. NiO sensor responses versus operating temperature for 5 ppm NO₂ and 100 ppm CO.

This behavior can be expected from follows the conventional metal oxide semiconductor theory and is generally observed on metal oxide-based semiconductor sensors. NO₂ is a highly reactive species showing an oxidizing character with respect to non-stoichiometric metal oxide. When NO₂ adsorbs on the NiO surface creates acceptor surface states. At room temperature, the main products of reaction of NO₂ with polycrystalline NiO are adsorbed NO₃. The Ni-NO₂ interactions on NiO are strong and Ni sites probably get oxidized and nitrated as a result of them. NO₂ is very efficient for fully oxidizing metal centers that are missing O neighbors in oxide surfaces [40].

This results in increased band bending at the grain surface and thus a rise in resistance and therefore low temperature detection is observed. With reducing gases, the gas detection mechanism is modulated by the presence of oxygen surface concentration that, with the increase of the temperature, leads to the higher interaction with the reducing gas. The oxygen from the air is chemisorbed as O₂⁻, O⁻ and O₂²⁻ on the surface thus decreasing the concentration of electrons near the surface and arising in a depletion layer of higher resistance. When exposed to a reducing gas, the co-adsorption and mutual interaction between the gas and the adsorbed oxygen result in oxidation at the surface and in a decrease of chemisorbed oxygen concentration, inducing an increase of the conductance.

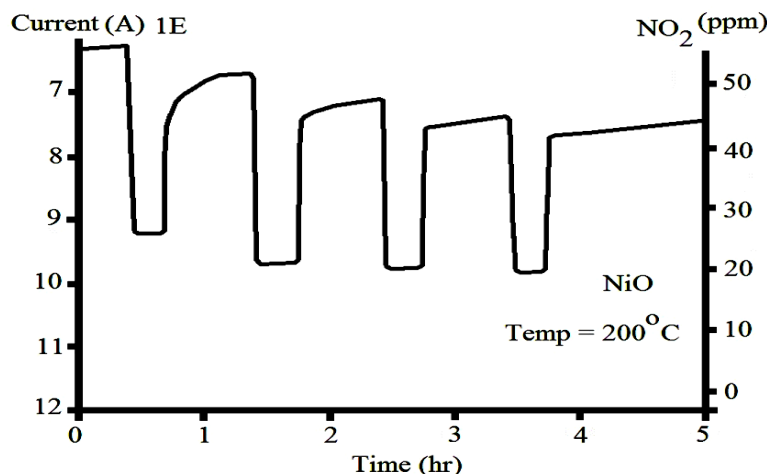


Figure 7. Dynamic responses of NiO Nano-crystals exposed to different NO₂ concentration at working temperature of 200 °C.

Fig. 7 reports the dynamic response of the NiO based sensor to a sequence of different NO₂ concentrations at 200 °C. The sensor appears to be very sensitive to NO₂. In fact, the responses of the sensor towards different concentrations of NO₂ are high and they cover several magnitude orders of current. However, the recovery time of the sensors after the exposure to the gas is slow, so the baseline does not return to the initial value. It seems that this drift is due mainly to the interaction of NO₂ gas and probably depends by the interactions mechanisms involved.

In fact, irreversible and slow reactions with chemical species in the ambient can cause this instability. The responses towards CO Fig. 8 are fast and reversible; the sensor provides a very stable signal and reaches its original baseline after each gas exposure cycle has been completed. The obtained responses seem to be comparable to NiO conductive-type thin and

thick films based sensors and even better in the case of NO₂ gas sensing tests. A comparison of the gas sensing capabilities of NiO-NP based gas sensors with some different NiO nanostructures based sensors reported in literature points out that the use of NiO at bulk size as sensing layer for chemical gas sensors leads to realize devices with higher sensitivity and stability than sensing layers of polycrystalline NiO films.

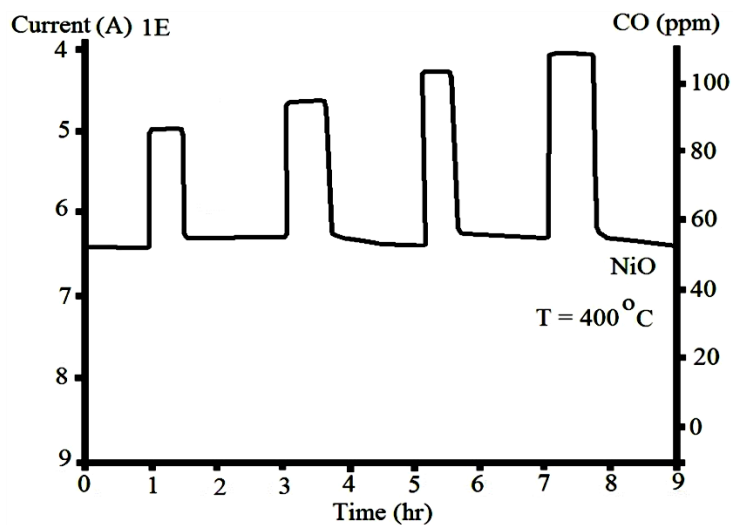


Figure 8. Dynamic responses of NiO Nano-crystals exposed to different CO concentration at working temperature of 400 °C.

In fact, despite the difference in morphology, the different properties due to the deposition techniques and device realization procedures employed, all the NiO nanostructures based sensors show important performances, principally high sensitivity, ascribed to a larger surface-to-volume ratio, and high stability due to the generally more stable single crystalline nanoparticles.

4 Conclusions

NiO Nano-crystals were synthesized at room temperature using a simple sonochemical method. The mean crystallite size of the obtained Nano-sized was found in the range from 20 to 150 nm. Dropcasting of the Nano-crystals onto alumina substrates allowed the fabrication of chemoresistive gas sensing devices. The gas sensing test on resulting devices show remarkable response to NO₂ even at very low operating temperatures and good responses towards CO.

This result is attributed to the preparation of highly Nano-sized oxide particles and to their processing for the device realization. In fact, the final sensing layer results a porous and not sintered structure resulting in extensive interaction with the gases. The results obtained are very promising and stimulating and in further developing of NiO-NP based sensor devices.

Acknowledgements

Supporting of this investigation by Lorestan University (Khorramabad, Islamic Republic of Iran), Baqiyatallah University Medical of Science and Kimya Javid Company, Gitipasand Industrial group, (Isfahan, Islamic Republic of Iran).

References

- [1] C.B. Murray, C.R. Kagan, M.G. Bawendi, *Annu. Rev. Matter Sci.* 30 (2006) 545.
- [2] G.-M. Chow, N. Ivanova Noskova, *Nano-structured Materials Science and Technology*, Kluwer Academic publishers, Dordrecht, 1998.
- [3] L. Mazzola, *Nat. Biotechnol.* 21 (2003) 1137.
- [4] R. Paul, J. Wolfe, P. Hebert, M. Sinkula, *Nat. Biotechnol.* 20 (2003) 277.
- [5] G. Blaser, T. Ruhl, C. Diehl, M. Ulrich, D. Kohl, *Physica A: Statistical and Theoretical Physics* 266 (1999) 218–223.
- [6] G. Korotcenkov, *Sensors and Actuators B* 107 (2005) 209–232.
- [7] B. Levy, *Journal of Electroceramics* 1 (1997) 239–272.
- [8] J. Bandara, C.M. Divarathne, S.D. Nanayakkara, *Solar Energy Materials and Solar Cells* 81 (2004) 429–437.
- [9] J. Bandara, J.P. Yasomane, *Semiconductor Science and Technology* 22 (2007) 20–24.

- [10] C.L. Liao, Y.H. Lee, S.T. Chang, K.Z. Fung, *Journal of Power Sources* 158 (2006) 1379–1385.
- [11] B. Pejova, T. Kocareva, M. Najdoski, I. Grzdanov, *Appl. Surf. Sci.* 165 (2000) 271.
- [12] H. Sato, T. Minami, S. Takata, T. Yamada, *Thin Solid Films* 236 (1993) 27.
- [13] K. Liu, M. Anderson, *J. Electrochem. Soc.* 143 (1996) 124.
- [14] V. Srinivasan, J. Weidner, *J. Electrochem. Soc.* 144 (1997) L210.
- [15] S.F. Wang, F. Gu, M.K. Lu⁺, *Langmuir* 22 (2006) 398.
- [16] Jin-Zhong Xu, Shu Xu, Jun Geng, Gen-Xi Li, Jun-Jie Zhu, *Ultrason. Sonochem.* 13 (2006) 451.
- [17] Sheng-Yi Zhang, Y. Liu, X. Ma, Hong-Yuan Chen, *J. Phys. Chem. B* 110 (2006) 9041.
- [18] H. Lei, Y.-J. Tang, J.-J. Wei, J. Li, X.-B. Li, H.-L. Shi, *Ultrason. Sonochem.* 14 (2007) 81.
- [19] V.G. Kumar, K.B. Kim, *Ultrason. Sonochem.* 13 (2006) 549.
- [20] Chang-Jie Mao, Hong-Cheng Pan, Xing-Cai Wu, Jun-Jie Zhu, Hong-Yuan Chen, *J. Phys. Chem. B* 110 (2006) 14709.
- [21] K.S. Suslick, M. Fang, T. Hyeon, *J. Am. Chem. Soc.* 118 (1996) 11960.
- [22] H. Zhou, Z. Zhou, *Solid State Ionics* 176 (2005) 1909.
- [23] Q.S. Song, Y.Y. Li, S.L.I. Chan, *J. Appl. Electrochem.* 35 (2005) 157.
- [24] J. Zhu, Z. Lu, S.T. Aruna, D. Aurbach, A. Gedanken, *Chem. Mater.* 12 (2000) 2557.
- [25] J.C. Yu, J. Yu, L. Zhang, W. Ho, *J. Photochem. Photobiol. A: Chem.* 148 (2002) 263.
- [26] L. Jiang, G. Sun, Z. Zhou, S. Sun, Q. Wang, S. Yan, H. Li, J. Tian, J. Guo, B. Zhou, Q. Xin, *J. Phys. Chem. B* 109 (2005) 8774.
- [27] M.J. Madou, S.R. Morrison (Eds.), *Chemical Sensing with Solid State Devices*, Academic Press, New York, 1989.
- [28] A. Vancu, R. Ionescu, N. Bârsan, in: P. Ciureany, S. Middelhoek (Eds.), *Thin Film Resistive Sensors*, IOP Publishing Ltd., 1992, p. 437 (Chapter 6).
- [29] S. Capone, *P. Encyclopedia of Nanoscience and Nanotechnology*, vol. 3, American Scientific Publishers, 2004, pp. 769–804.
- [30] Y. Shimizu, M. Egashira, *MRS Bull.* 6 (1999) 18–24.
- [31] G. Neri, A. Bonavita, G. Rizzo, S. Galvano, N. Pinna, M. Niederberger, S. Capone, *P. Sens. Actuators B* 122 (2007) 564–571.
- [32] E. Comini, *Anal. Chim. Acta* 568 (2006) 28–40.
- [33] C. Xu, J. Tamaki, N. Miura, N. Yamazoe, *Sens. Actuators B* 3 (1991) 147.
- [34] N. Yamazoe, *Sens. Actuators B* 5 (1991) 7–19.
- [35] N. Bârsan, M. Schweizer-Berberich, W. Göpel, *Fresenius J. Anal. Chem.* 365 (1999) 287.
- [36] L.F. Dong, Z.L. Cui, Z.K. Zhang, *Nanostruct. Mater.* 8 (7) (1997) 815–823.
- [37] H. Gong, H. J.Q., J.H. Wang, C.H. Ong, F.R. Zhu, *Actuators B* 115 (2006) 247–251.
- [38] K. Soulantica, L. Erades, M. Sauvan, F. Senocq, A. Maisonnat, B. Chaudret, *Adv. Funct. Mater.* 13 (2005) 553–557.
- [39] M. Epifani, E. Comini, J. Arbiol, R. Diaz, N. Sergent, T. Pagnier, P. Siciliano, G. Faglia, J.R. Morante, *Sens. Actuators B* 130 (2008) 483–487.
- [40] J.A. Rodriguez, T. Jirsak, J. Dvorak, S. Sambasivan, D. Fisher, *J. Phys. Chem. B* 104 (2000) 319–328.